Effects of hydrolysis processing on the character of forsterite gel fibers. Part II: crystallites and microstructural evolutions

M.T. Tsai*

Department of Materials Science and Engineering, National Huwei Institute of Technology, PO Box 385 Touliu, Yunlin 640, Taiwan

Abstract

Crystallites and microstructural evolutions of the three forsterite fibers derived from three different precursor sols were compared. The formation of crystalline forsterite commenced at a temperature as low as 550 °C in all the fibers. Gel fiber prepared with excess ethanol showed a lower homogeneity and densification; a second phase of magnesia was observed on heating. The water content also affected the grain size and homogeneity of the fired fibers. On heating at 1100 °C, the three forsterite fibers were microporous with grain sizes less than 0.1 µm; further heating at 1300 °C resulted in grain growth up to 0.3–0.5 µm and denser microstructures, depending on the amount of water and ethanol. © 2002 Elsevier Science Ltd. All rights reserved.

Keywords: Crystallites; Fibres; Forsterite; Mg₂SiO₄; Microstructure

1. Introduction

Forsterite (Mg$_2$SiO$_4$) is an intermediate compound in the MgO–SiO$_2$ system, in addition to being an insulator at high frequencies, it is also able to be used as a refractory because of high melting temperature of about 1890 °C.[1] The crystal structure of forsterite is orthorhombic with space group pbnm, which could be regarded as consisting of SiO$_4$ tetrahedral linked together by MgO$_6$ octahedral.[2,3] In general, fibers having high porosity are useful as catalyst supports but for high mechanical properties (i.e. strength and modulus) it is necessary to attain uniform and fine-grained microstructures.[4]

It is widely recognized that the sol-gel process can provide molecular-level mixing for a high degree of homogeneity, which leads to lowering of the crystallization temperature and prevents phase segregation during the thermal treatment.[5,6] However, in multicomponent silicate systems, the hydrolysis and condensation rates are different between silicon and the other alkoxides. This may result in chemical inhomogeneity of the gels, leading to higher crystallization temperature and undesired

crystalline phases.[6] Several approaches have been used to overcome this limitation, including slow additions of water,[7] partial prehydrolysis of the silicon alkoxide,[7] and synthesis of multi-cation alkoxides or chemical modification with chelating ligands.[6,8] Since the hydrolytic polycondensation rates of magnesium and silicon alkoxides are substantially different, homogeneous magnesium silicate gels would not readily be formed by the hydrolysis of the alkoxide mixtures. Homogeneous forsterite xerogels and powders have been prepared by sol-gel process[9,10] using partial prehydrolysis and slow additions of water routes. In part 1 of this study,[11] however, it has been shown that this problem can also be solved by using proper amount of acetic acid, water, and ethanol to control the hydrolytic condensation reaction, consequently homogeneous, clear sols and transparent gel fibers can be obtained.

A previous study[11] has already shown that the content of water and ethanol significantly affect the properties of the sols and the dried gel fibers, e.g. spinnability, length, morphology, and molecular structures, for a given composition condition with the optimum amount of acetic acid. In the present study, the crystallites and the microstructural evolutions of these gel fibers are investigated and qualitatively described, in order to approach the effects of water and ethanol.

---

* Tel.: +886-5-5320731; fax: +886-5-6328863.
E-mail address: mttsai@ms23.hinet.net

2. Experimental procedure

Three batches of forsterite precursor gel fibers were prepared from the three spinnable sols with different water and ethanol content. TEOS ($Si(OC_2H_5)_4$) and magnesium methoxide ($Mg(OCH_3)_2$) were used as the starting materials; the procedure for preparing the spinnable sols and the gel fibers were described in detail in the previous report.[11] The optimum molar ratio of acetic acid was 1.0 to TEOS for all the solutions investigated. Three gel fibers were derived from the solutions with the molar ratio of water: ethanol: TEOS which were 0.5:3:1 (labeled as fiber F1), 2:3:1 (labeled as fiber F2), and 0.5:20:1 (labeled as fiber F3), respectively; the relative sols and characteristics have been shown in the previous report.[11] The gel fibers were drawn from the spinnable sols and followed drying at room temperature.

The crystallization process of fibrous gel was studied by differential thermal analysis (DTA) and thermogravimetry (TG; Seiko SSC 5000), powder X-ray diffractometry (XRD; Rigaku D/MAX-III), and Fourier transform-infrared spectrometry (FT–IR; Bomen Michelson MB100). Thermal analysis was performed on gel fibers that were broken into fragments, and the measurement was conducted in flowing air at a heating rate of 10 °C min^{-1}. Infrared spectra of dried and heated fibers were recorded in the 450–2000 cm^{-1} frequency range with 2 cm^{-1} precisions using a constant powder sample imbedded in 200 mg KBr pellet. For IR and XRD samples, fibrous gels were dried at 60 °C in air and then were heated at 200–1300 °C for 2 h at a heating rate of 10 °C min^{-1} followed by grinding into fine powders for the measurements. The microstructures of the fired fibers were observed by scanning electron microscopy (SEM; JSM-T330 Jeol and Hitachi-S 4500), where the gel fibers were heated at 1100–1300 °C in air using a rate of 3 °C min^{-1}. Specific surface area was performed on the fired fibers without crushing by a Brunauer-Emmett-Teller (BET) measurement, using a surface area analyzer (Micromeritics ASAP 2400). The dielectric constant was measured at 1 MHz by a precision inductance–capacitance–resistance (LCR) meter (HP 4284A) with silver electrodes attached to both ends of a fiber; for comparison, disk samples were uniaxially pressed from the relative gel-derived powders to obtain dielectric properties. The tensile strength was measured by an Instron-type testing machine on a single fiber filament with a gauge length of 10 mm, using a technique similar to that described by Kamiya and Yogo;[12] the force required to fracture the fiber was measured using a transducer load cell and the fiber diameter was measured using optical or scanning electron microscopy. Several fiber specimens of each composition were measured for above properties to obtain an average value.

3. Results and discussion

3.1. Crystallization of gel fibers

3.1.1. IR spectrum

The infrared spectrum of the processed gel fibers F1, F2, and F3 heated at various temperatures for 2 h were given in Figs. 1–3. The spectra of the dried gel fibers have been characterized in the previous report.[11] The infrared spectra on heating these gel fibers indicated that a further condensation might occur between the silanol groups and the decomposition of acetate ligand groups. Continued condensation with temperature was evidence from the reduction in the relative intensity of the bands around 910 and 860 cm^{-1} assigned to Si–OH stretching[13,14] along with a progressive decrease in the intensity of the characteristic peaks of acetate ligands around 1500 cm^{-1}, as shown in Fig. 1. For fiber F1, the band around 1637 cm^{-1}, due to adsorbed water,[13] and the bands at 1688 and 1348 cm^{-1}, assigned to residual acetic acid or unidentate acetate,[15,16] and the bands around 660 and 625 cm^{-1}, associated with the vibration modes of OCO and COO,[17] decreased in intensity with increasing temperatures and eventually vanished at 400 °C, this probably reflected the loss of organic acid and the decomposition of residual organics. The doublets of acetate ligands also showed a progressive decreased upon heating. A residue doublet was still
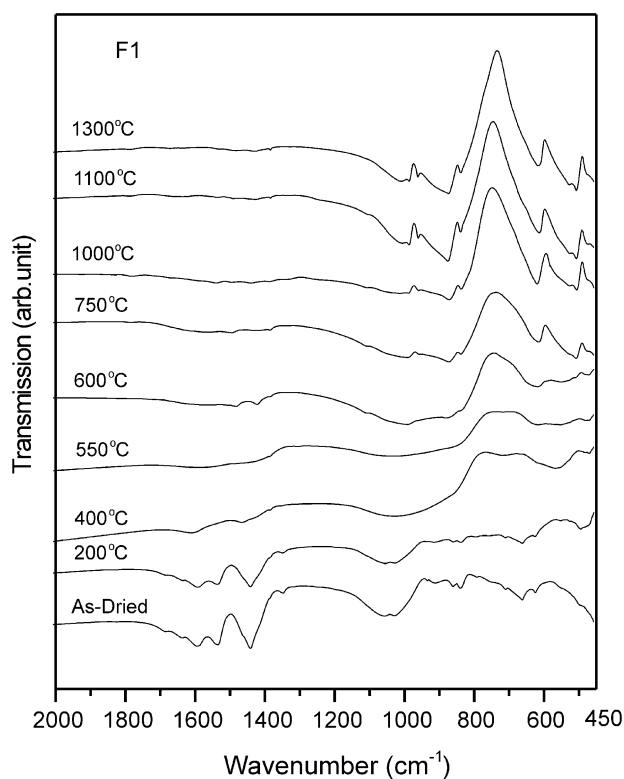

Fig. 1. Infrared spectra of the processed gel fiber F1 heated at various temperatures for 2 h.

visible between 1610 and 1465 cm^{-1} on heating at 400 °C, which might be correlated with the residue bridging acetates,[15,16] and no longer clear after heating at 550 °C. Most of the peak related to the Si–O$^-$ bonds also decreased in the intensity upon heating. The peaks corresponding to Si–O–Si asymmetry stretching vibration at 1055 and 1025 cm^{-1}, decreased in the intensity and shifted those bands to lower wavenumbers with increasing temperatures and gradually disappeared at above 400 °C, a similar result was also observed in fibers F2 and F3, as shown in Figs. 2 and 3. This effect should be associated with the rearrangements of the Si–O–Mg linkages in the fibrous gel structures.

Fig. 1 also revealed a progressive transformation the gel structure toward the crystallization of forsterite and suggested that the rearrangements of Si–O–Mg bonds might occur. A weak shoulder around 550 cm^{-1}, presumably assigned to the modes of MgO_4 in the Si–O–Mg linkages,[11,18,19] shows an increase in the intensity up to 400 °C. At the same time, the band due to SiO_4 bending[18] around 496 cm^{-1} also increased in intensity at 200 °C and substantially decreased at 400 °C; instead, appearing a broad band with stronger absorption around 568 cm^{-1} and a new peak around 470 cm^{-1} corresponding to MgO_6 modes.[2,3] This trend might be associated with the rearrangements of Si–O–Mg linkages and the coordination of Mg^{2+}. Further heating at 550 °C, the band around 568 cm^{-1} decreased in intensity

but the band around 470 cm^{-1} retained the same position, and some of the characteristic peaks of crystalline forsterite[2,3] started to show at around 472, and 616 cm^{-1}. On further heating at 600 °C, those peaks due to crystalline forsterite became more obvious. Meanwhile, the bands corresponding to C–H vibration modes around 1385, 1422 and 1483 cm^{-1} were visible, which were mainly due to the combustion of the organic groups;[13,20] the traces of these bands could still be detected at higher temperatures. Above 750 °C, the bands related to the characteristic peaks of well-crystallized forsterite appear at 1007, 986, 960, 873 and 838 cm^{-1} (SiO_4 stretching), at 616, 527 and 507 cm^{-1} (SiO_4 bending), and at 475 cm^{-1} for modes of octahedral MgO_6; band positions for forsterite agreed with the results of previous investigations.[2,3]

Similar features were observed for gel fibers F1 and F3, as given in Figs. 2 and 3. Upon heating at 750 °C, the characteristic peaks of crystalline forsterite clearly appeared, and the crystallinity of forsterite increased with temperature. Fig. 2 displayed the characteristic peaks of acetate ligands in fiber F2 and also decreased in the intensity with heating and gradually disappeared at 750 °C; instead, the bands related to the characteristic peaks of well-crystallized forsterite[2,3] appeared at 987, 961, 875 and 838 cm^{-1} (SiO_4 stretching), at 616, 528 and 508 cm^{-1} (SiO_4 bending), and at 477 cm^{-1} (MgO_6 modes). After heating at 1000 °C, a shoulder at 662
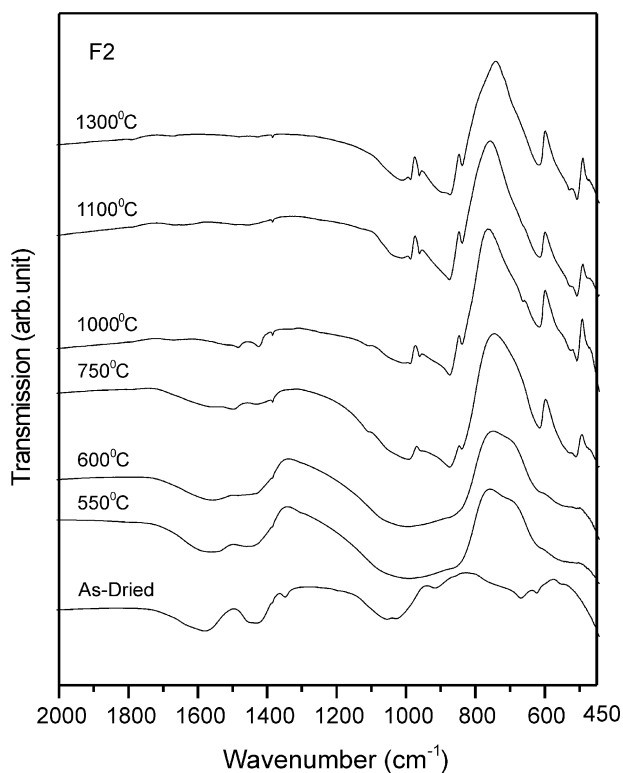

Fig. 2. Infrared spectra of the processed gel fiber F2 heated at various temperatures for 2 h.
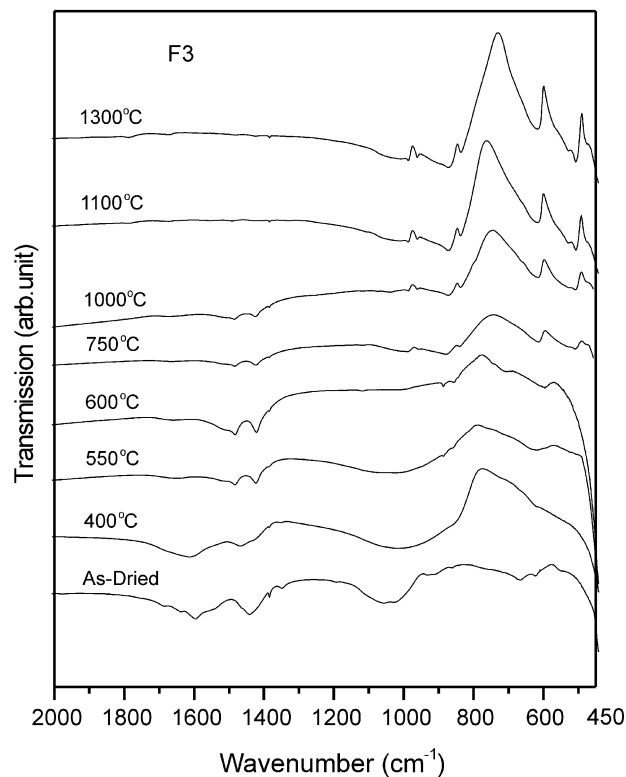
Fig. 3. Infrared spectra of the processed gel fiber F3 heated at various temperatures for 2 h.

cm^{-1} was associated with the vibration modes of Mg–O,[21] which was not the characteristic peak of forsterite and disappeared above 1100 °C, as presented in Fig. 2. Similar results of the progressive transformation of the gel structure toward the crystallization of forsterite were observed in Fig. 3 for fiber F3. However, those bands due to the combustion of the organic groups around 1385, 1422 and 1483 cm^{-1} were also clearly visible even heated at 1000 °C for both fibers F2 and F3; this phenomenon was more prominent in fiber F3 when heated at 550–1000 °C, as shown in Fig. 3. This result indicated that the decomposition and burn-off of the residue organics proceeded throughout the heating process, thus, a higher heating temperature or preheating treatment was required in order to burn off the residual organics.

3.1.2. XRD studies

X-ray diffraction studies revealed some important information regarding phase evolution and chemical homogeneity of the samples. Figs. 4–6 show the X-ray diffraction patterns of the processed gel fibers that were essentially amorphous after drying, and the formation of forsterite crystallite commenced at a temperature as low as 550 °C in all the samples; however, the transformation being practically complete at above 750 °C. For specimen F1, the fibers remained amorphous after drying and heating at 400 °C; with a further heating at
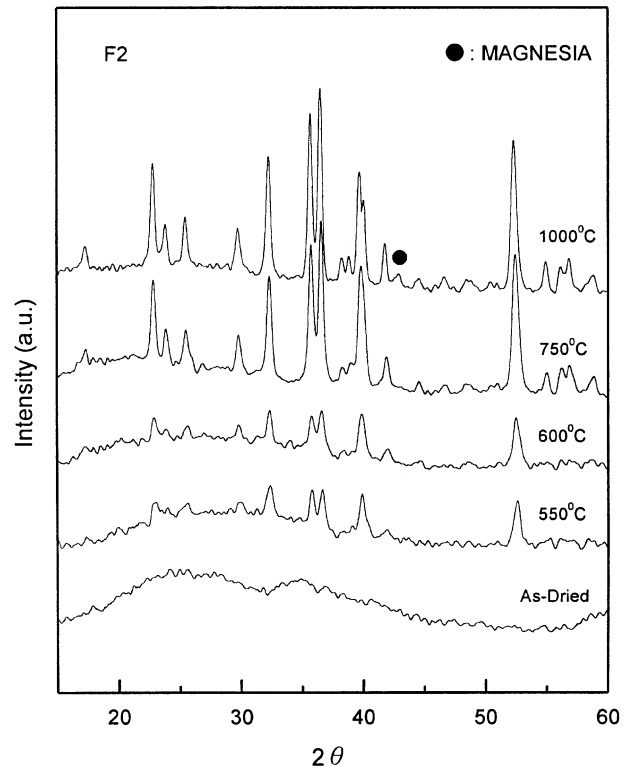

Fig. 5. X-ray diffraction patterns of fibrous gel F2 fired at various temperatures for 2 h.
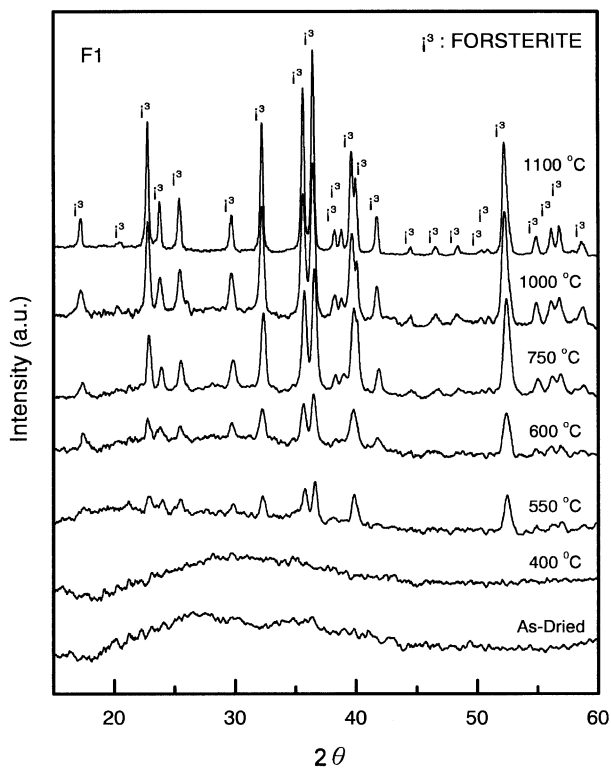

Fig. 4. X-ray diffraction patterns of fibrous gel F1 fired at various temperatures for 2 h.
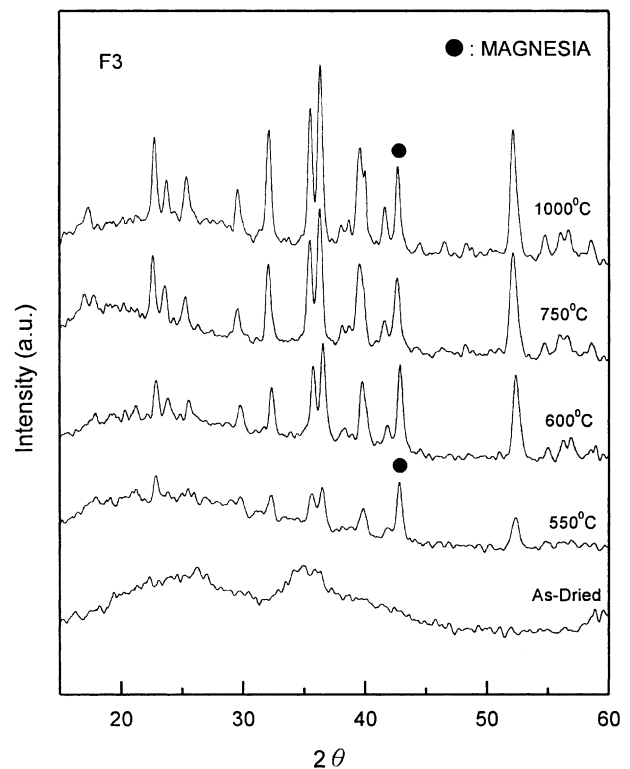

Fig. 6. X-ray diffraction patterns of fibrous gel F3 fired at various temperatures for 2 h.

550 °C, it crystallized directly into a single phase of forsterite[22] without the formation of an intermediate phase, as depicted in Fig. 4; it also displayed that the crystallinity of forsterite increased with heat-treatment temperatures up to 1000 °C, in which forsterite was the dominated phase. This result was consistent with the appearance of the characteristic peaks of crystallite forsterite in the IR spectrum, as was depicted in Fig. 1. In contrast, specimen F2 also showed similar trends but a trace of MgO (200) peak[23] was detected for the fibers on heating at 1000 °C, as shown in Fig. 5; this trace of magnesia phase disappeared after further heating at 1100 °C, and only forsterite phase was observed. This result was consistent with the observation of infrared spectra, as the band at 662 cm^{-1} was presented in Fig. 2. The result might reflect a better homogeneity and reproducibility in the mixing scale of Mg–Si components in gel fiber F1 compared to fiber F2. However, the peak of magnesia phase was observed clearly at 550 °C for specimen F3 as shown in Fig. 6, a trace persisting even at heating above 1000 °C. This result revealed a higher inhomogeneity in the mixing scale of Mg–Si components in gel fibers F3. The processed gel fibers showed the difference in the chemical homogeneity during heating, which probably resulted from the different solution concentrations in the precursor solutions. The content of water and ethanol apparently played important factors not only in controlling the length of drawn fibers but also in the homogeneity of the crystalline phase.

In the chemical solution route, molecular-level mixing is important for lowering the crystallization temperature and for preventing the phase segregation during heating of the products.[18] From the fact that, the appearances of the three spinnable sols were homogeneous and clear and the formation of glass-liked transparent gel fibers in all the cases were investigated. It was reasonable to expect that both magnesium and silicon ions were uniformly distributed in those fibrous gel structures. The low crystallization temperature shown in Figs. 4–6 might be partly responsible for the three gel fibers with the intimate mixing at the molecular level in their polymeric structures.

However, X-ray studies exhibited that there essentially existed a different level of homogeneity and/or ultrastructures in these gel fibers after heating. Namely, this result suggested that the higher water and ethanol content, especially the effect of the latter, would probably lead to the local nonuniform distribution of Mg and Si in the Si–O–Mg linkages and metal acetate complexes of the polymer backbones, and subsequently the formation of MgO clusters to be crystallized on heating. The reason was not understood clearly, but might be interpreted as follows. For the case of dilute with ethanol (i.e. for fiber F3), since the amount of water in the precursor solution was small, a transesterification reac-

tion between magnesium methoxide and ethanol thus might be taken into account. In the sol-gel process, transesterification could occur when alkoxides were hydrolyzed in alcohol containing different alkyl groups.[24] It might be conjectured that if partial substitution of ethyl groups for methyl groups in magnesium methoxide were made, which would produce more extent of partial hydrolyzed of magnesium alkoxide derivatives compared to the solution with lower ethanol (i.e. for fiber F1), because the reactivity or hydrolysis rate of the ethoxide groups was lower than the methoxide groups.[5] This result would promote the partial hydrolyzed species undergoing self-condensation during firing. This was reflected on the presence of a magnesia phase after heating at 550 °C, as shown in Fig. 6. The higher water seemed to also influence the reproducibility of homogeneous forsterite, meaning that the occurrence of local chemical inhomogeneity was possible when the gel fibers were prepared such conditions. Certainly, however, the drawbacks could be avoided, if less content of ethanol and water were used, and homogeneous forsterite fibers with good reproducibility might result.

3.1.3. Thermal analysis

Fig. 7 gives a comparison of the TG and DTA curves for the three gel fibers previously dried at room tem-
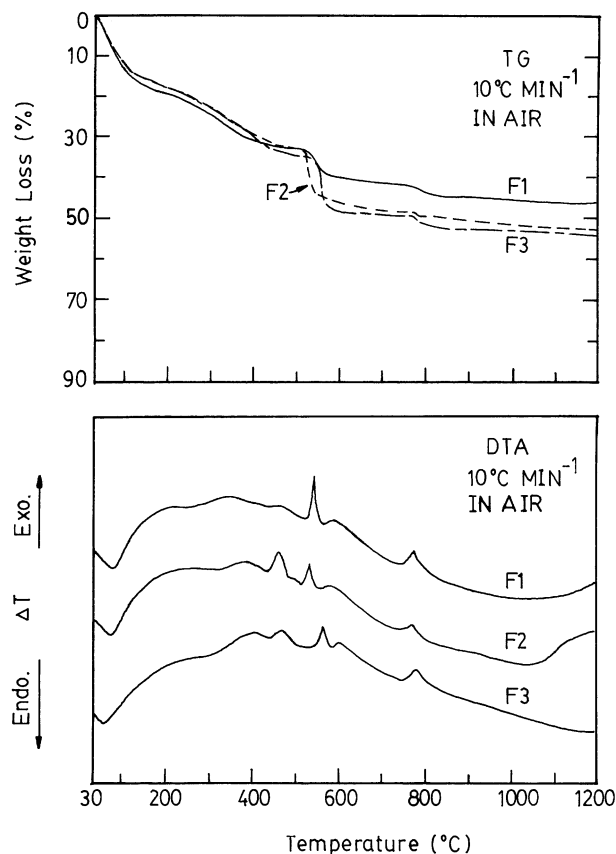

Fig. 7. TG and DTA curves for fibrous gels F1, F2 and F3 pre-dried at room temperature.

perature. Similar features of the curves could be seen in those specimens. Four distinct steps of weight loss were observed on all three of the TG curves, which were around 30–180, 200–500, 510–620, and 770–820 °C, respectively. One mainly endothermic peak and four mainly exothermic peaks were also observed on all of the DTA curves. For specimen F1, the mainly endothermic peak was around 72 °C, and the exothermic peaks were around 320, 450, 546 and 779 °C, respectively; these peaks were also clearly observed at around 69, 402, 470, 538 and 781 °C for specimen F2, and were around 65, 411, 480, 566 and 786 °C for specimen F3, respectively.

For specimen F1, the first weight loss around 30–180 °C was mainly due to the evaporation of water, free acetic acid or residual organics corresponding to a broad endothermic peak around 72 °C on the DTA curve. The second around 200–500 °C involved about 13.8 wt.% weight loss and a small endothermic peak around 250 °C, following by a broad exothermic peak around 320 °C and a small one around 450 °C. Similar behaviors were observed in specimens F2 and F3 but of two prominent exothermic peaks around 402 and 470 °C for the former, as well as 411 and 480 °C for the latter. Fiber specimen F1 seemed to decompose at a lower temperature than the others. This step might be due to the liberation of hydroxyl groups, alcohol and acetate groups, and their combustion. This is consistent with the results of IR spectra, indicating that continued condensation with temperature could occur between silanol groups and decomposition of acetate ligand groups. The third step around 510–620 °C involved about 8.5 wt.% significant weight loss and also accompanied a sharp exothermic peak around 546 °C on the DTA curve of specimen F1, similar trends were also observed in specimens F2 and F3 but with a higher weight loss. According to the results of X-ray diffraction, the crystallization of the forsterite phase began at 550 °C for the three specimens; moreover, IR spectrum showed the bands of acetate ligands decreased in intensity along with the disappearance of the bands of silanol groups and the stretching modes of Si–O–Si upon heating at 550 °C; in addition, infrared spectra also revealed that the combustion and decomposition of residual organic groups occur at 400–600 °C, as peaks appeared around 1385, 1422 and 1483cm^{-1}. From these results, the third step suggested that the combustion of residual organic groups and the further condensation reaction could induce the conversion of the amorphous gel fibers into crystalline forsterite. The fourth step around 770–820 °C involved a small weight loss of about 1.4–2.3 wt.% and an exothermic peak around 779–786 °C on the DTA curves of the three specimens; this step might be considered as the combustion and the removal of residual C–H groups still proceeded during firing, as indicated in the IR spectra. A gradual and slight weight loss was

continued up to 1200 °C in the three specimens. These transparent gel fibers turned black at heating above 200 °C and then white after 1000 °C, may be also in favor of above observation.

The thermal analysis did not show any evident difference between the three gel fibers. Namely, these gel fibers could be regarded as essentially similar in their thermal reactivity. However, the examination of X-ray diffraction patterns suggested that there existed a difference in micro- or nanohomogeneity of these gel fibers although the crystallinities were similar in all the cases investigated. Gel fiber prepared with excess ethanol implied the green structure had a lower homogeneity in the mixing scale of Mg–Si components than the others. The local chemical inhomogeneity was observed in fiber F3 during heating, as confirmed by XRD study.

3.2. Microstructural evolution

Fig. 8 shows scanning electron micrographs of the fibers after heating at 1100 °C. As shown, all the fired fibers exhibited porous on the fracture surfaces and presented a few cracks on the surfaces; in which the fired fiber F2 exhibited a relative denser structures of the surface compared to the others. Under higher magnification, as illustrated in Fig. 9, the observed microstructures of these fired fibers clearly revealed that many small pores retained in fibers F1 and F3, and the latter contained larger pores, as given in Fig. 9a and c, whereas a relatively denser microstructure of fiber F2 could be seen in Fig. 9b. Upon heating at 1100 °C, these fired fibers also exhibited fine-grained structures. As shown in Fig. 9d, fiber F1 presented nanocrystalline of about 50–100 nm in size; the average grain size of the fired fiber F1 was about 90 nm determined using the linear intercept method.[25] Both fibers F2 and F3 also contained quite small grain sizes of about less than 0.1 μm, as given in Fig. 9b and c. The results revealed that the obtained forsterite fibers were microporous with nanocrystalline grain size on heating at 1100 °C. The microporous structures of fired fibers might mainly result from the removal of the volatile species, e.g. water and organic groups, and/or the liberation of gas evolved by combustion of organic groups.

Increasing the heating temperatures to 1300 °C, a relatively denser microstructure with submicrometer grains of the three fibers were illustrated in Fig. 10. The three fibers showed evident differences in morphology of firing at 1300 °C compared to those of firing at 1100 °C. The surface and fracture surface of fiber F1, as shown in Fig. 10a, were denser after heating at elevated temperature; moreover, a more uniform surface was observed in contrast to fibers F2 and F3. Both fibers F2 and F3, as shown in Fig. 10b and c, also had a dense cross-section, but the surface of fiber F2 became somewhat rough and presented some defects such as cracks and flaws in the
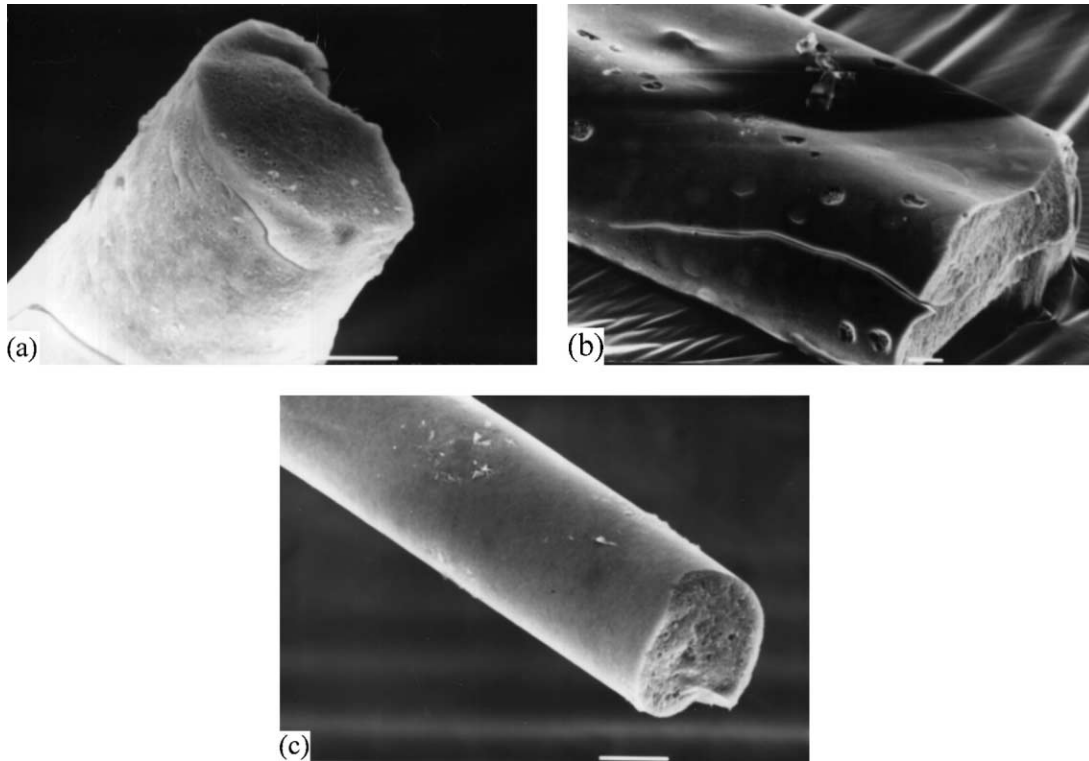
Fig. 8. Scanning electron micrographs of processed gel fibers (a) F1, (b) F2 and (c) F3 heat-treated at 1100 °C for 2 h. Bars = 10 µm.
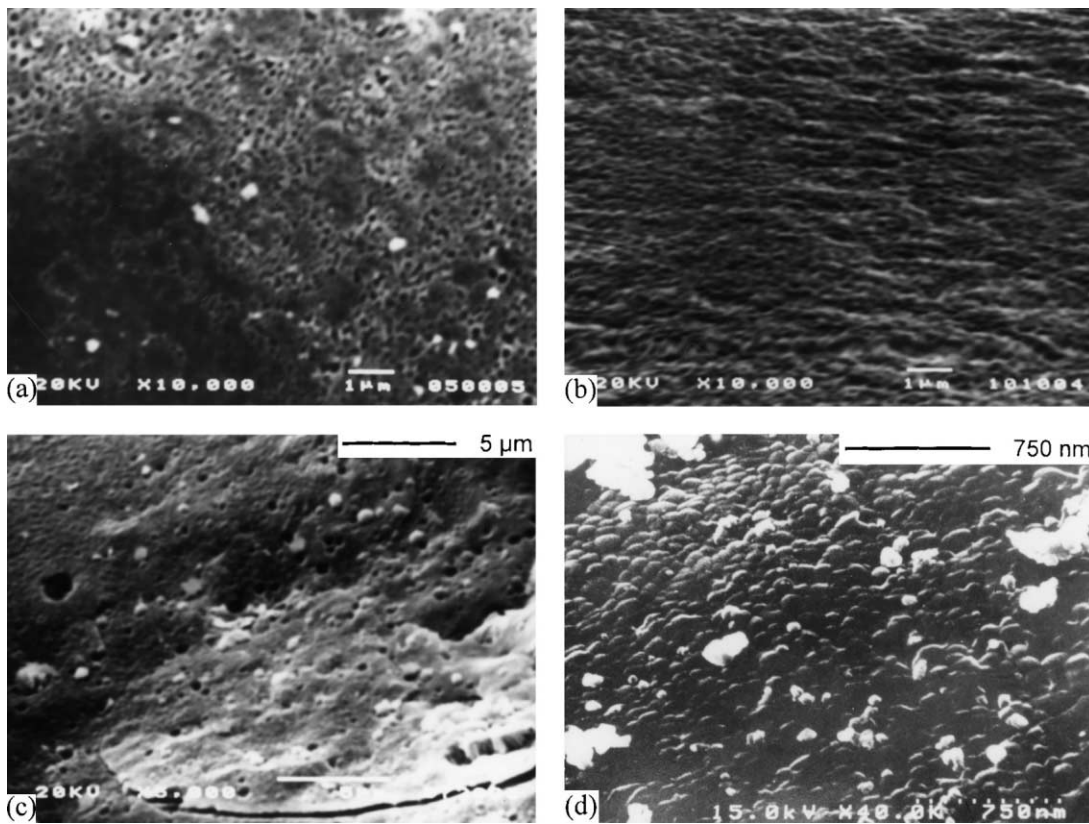

Fig. 9. Higher magnification SEM micrographs of processed forsterite fibers (a) F1, (b) F2 and (c) F3 heated at 1100 °C for 2 h, showing the microporous structures; (d) is a higher magnification of (a), indicating the fine-grained microstructure.

cross section. For fiber F3, a nonuniform surface and some bubbles on the cross-section were observed. The observed defects in the fired fibers could be ascribed to the combustion of the residual organics and the removal of the volatile substances, as were described previously[12,26,27] on the gel-derived fibers. Since the gel fiber became stiff and denser on heating, expelling the volatile substances out of the solidified gel fibers at higher temperature might produced some defects such as cracks, bubbling or nonuniforitty on the surface and cross-section. The observation of cracks on the surface and cross-section of fiber F2 upon heating at 1100–1300 °C, which might be partly due to a more denser

green structure of the fiber. The green structure of fiber F2 was considered to be denser, the difficulty in removing the volatiles would be increased during heating, and thus the forced escape of the volatiles might leave some cracks on the surface and cross section of the fired fiber.[12]

In addition, grain growth evidently occurred upon heating at 1300 °C. As shown in Figs. 10d and e, the average grain sizes of fiber F1 and F2 were about 0.3 μm and about $\leqslant 0.5$ μm, respectively. This result suggested that the fiber derived from the higher water condition that had larger grain size after firing at 1300 °C, which was probably related to the green structures of
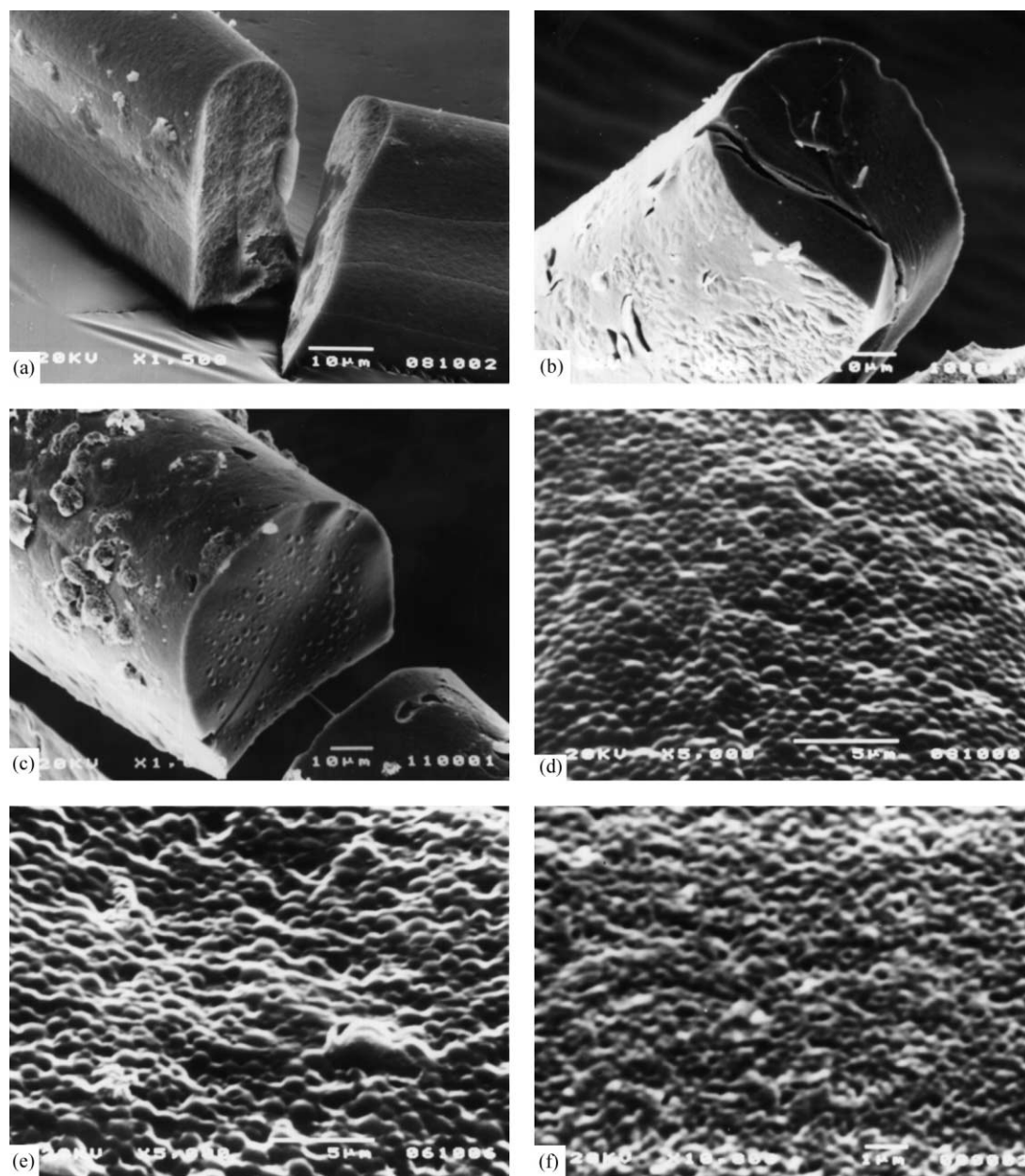

Fig. 10. Scanning electron micrographs of processed forsterite fibers (a) F1, (b) F2 and (c) F3 heated at 1300 °C for 2 h; (d), (e) and (f) are higher magnification of (a), (b) and (c), respectively, showing the microstructures of these fired fibers.

fiber F2 that were more branched and denser. In contrast, fiber F3 seemed to have the same average grain size as fiber F1 but of a porous microstructures, as given in Fig. 10f. The addition of excess ethanol into the precursor sol gave rise to shorter gel fibers; such fibers were relatively porous after firing. The excessive porosity in the fiber F3 probably resulted from the removal and burnout of a larger amount of organic species in contrast to fibers F1 and F2, giving rise to larger voids or pores. More weight loss was observed in gel fiber F3, as was shown in the thermal analysis, which might be in favor of the above assumption.

The decomposition and burn-off of the residual organics proceeded throughout the heating process, leading to densification or damage to the resultant forsterite fibers. The volatile components and the fibrous gel structures apparently could impact the morphologies of the fired fibers. It could be inferred that the volatile components remaining in the three gel fibers and their green structures were different because the gel fibers were derived from different solution conditions. The problem of making glass or ceramic fibers from the fibrous gels has been investigated by many studies.[12,26–29] Since fibrous gels contain large amounts of volatile matter, removal of the organic residues prior to the gel-to-ceramic conversion was important for obtaining uniform and dense structures. Many approaches have been proposed to improve the fired fibers, including preheating the gel fibers,[27] immediately heating the as-drawn fibers,[26] or reduced the heating rate[26,29] etc. The present study did not optimize the heating rate or pretreat the gel fibers, however, it was found that the densification of the fibers could be improved by heating at higher temperature. The influences of water and ethanol on the fiber prepared, which in turn influenced the morphology of the fired fibers were observed. The gel fibers prepared with higher water content (i.e. fiber F2) implied larger grain size in the resultant forsterite fibers, as compared to the fiber that derived from the low water condition (i.e. fiber F1). With excess ethanol, the obtained forsterite fibers were more porous as in the case of fiber F3. Accordingly, the content of water and ethanol exhibited the influences on the grain size and microstructural morphology of the forsterite fibers.

Some properties of the fired fibers are listed in Table 1. After heating at 1100 °C, the specific surface areas of forsterite fibers F1, F2 and F3 were about 22, 18 and 35 m^2/g, respectively. The tensile strength was in the range of 150–350 MPa for the fibers with diameters of about 20–50 μm. In contrast to fiber F1, it seemed that fiber F2 had a higher tensile strength in average, while fiber F3 had a lower strength; this might be largely due to fiber F3 with more porous microstructures. The tensile strength of the fired fibers was difficult to measure, because the fibers were too fragile to be handled easily without cracking. After heating at 1300 °C, the specific surface areas of the forsterite fibers F1, F2, and F3 decreased to about 9.6, 7.8 and 21 m^2/g, respectively. This result was consistent with the microstructural observation, meaning that the fiber structures became denser after heating at 1300 °C. The dielectric constant at room temperature of the fibers was in the range of about 6.4–7.2, at 1 MHz. These values were comparable to the respective bulk sample values of about 5.6–7.0. This result revealed the low dielectric characteristics of the three fibers. The values of the fiber strength in the present study were lower than those of the silicate fibers reported previously;[12,29] this probably due mainly to the existence of microporous of the forsterite fibers. In addition, the fiber strength decreased with increasing the diameters of the fibers investigated. The tensile strength of fired fibers decreased with increasing diameter could result from larger diameter retained more amount of cracks or pores. However, BET measurement also suggested the fibers obtained at 1100 °C that were microporous and thus low strength could result. The fibers described seem to be too weak to be of practical value even for non-structural application. Studies are now being carried out to improve the sinterability of these gel fibers by varying the heating conditions.

4. Conclusions

The chemical composition in the precursor solution greatly influenced the structures of the sols and the fibrous gels,[11] which in turn affected the homogeneity and microstructural evolution of the gel fibers on heating. Gel fiber prepared with higher water condition had larger grain size and a denser structure after heating at 1100–1300 °C, while gel fiber prepared with excess ethanol showed a more porous structure and a lower homogeneity. Proper adjustment of the content of water and ethanol was essential for preparing forsterite fiber with chemical homogeneity and with good reproducibility. On heating, homogeneous forsterite fiber with submicron grain size and low dielectric characteristic could be obtained.

Table 1
Specific surface area, dielectric constant and tensile strength of the fired fibers after heating at 1100–1300 °C for 2 h

Samples	Surface area (m^2/g)		Tensile strength (MPa)	Dielectric constant
	(1)[a]	(2)[a]	(1)	(2)
F1	22 (±0.2)	9.6 (±0.7)	180–320	6.8 (±0.7)
F2	18 (±0.3)	7.8 (±0.5)	170–350	7.2 (±0.6)
F3	35 (±0.8)	21 (±1)	150–290	6.4 (±0.7)

[a] (1) After heating at 1100 °C for 2 h, and (2) heating at 1300 °C for 2 h.

In this study, an important practical advantage of the use of acetic acid was that it enhanced the spinnability and the formation of clear sols; this lead to not only the gel fibers, but thin film and coating, as well, could also be prepared. However, the burnout of the organic species is still a problem to be solved. The formation of some defects e.g. cracks and pores, might lower the fiber strength. Further investigations are necessary to optimize the drying and the firing schedules for minimizing the pores or flaws formation.

Acknowledgements

References

1. Mitchell, M. B. D., Jackson, D. and James, P. F., Preparation of forsterite (Mg_2SiO_4) powders via an aqueous route using magnesium salts and silicon tetrachloride ($SiCl_4$). *J. Sol-Gel Sci. Technol.*, 1999, **15**, 211–219.
2. Jeanolz, R., Infrared spectra of olivine polymorphs: α, β phase and spinel. *Phys. Chem. Minerals*, 1980, **5**, 327–341.
3. Lan, P. K., Yu, R., Lee, M. W. and Sharma, S. K., Structural distortions and vibration modes in Mg_2SiO_4. *Am. Mineral.*, 1990, **75**, 109–119.
4. Marshall, D. B., Lange, F. F. and Morgan, P. D., High-strength zirconia fibers. *J Am. Ceram. Soc.*, 1987, **70**, c-187–c-188.
5. Mehrotra, R. C., Chemistry of alkoxide precursors. *J. Non-Cryst. Solids.*, 1990, **121**, 1–6.
6. Livage, J., Babonneau, F., Chatry, M. and Coury, L., Sol-gel synthesis and NMR characterization of ceramics. *Ceram. International*, 1997, **23**, 13–18.
7. Yoldas, B. E. and Partlow, D. P., Formation of mullite and other alumina-based ceramics via hydrolytic polycondensation of alkoxides and resultant ultra- and micro-structural effects. *J. Mater. Sci.*, 1988, **23**, 1895–1900.
8. Bradley, D. C., Mehrotra, R. C. and Gaur, D. P., *Metal Alkoxides*. Academic Press, New York, 1978 (pp. 299-308).
9. Burlitch, J. M., Beeman, M. L., Riley, B. and Kohlstedt, D. L., Low-temperature syntheses of olivine and forsterite facilitated by hydrogen peroxide. *Chem. Mater.*, 1991, **3**, 692–698.
10. Ban, T., Ohya, Y. and Tokahashi, Y., Low-temperature crystallization of forsterite and orthoenstatite. *J. Am. Ceram. Soc.*, 1999, **82**, 22–26.
11. Tasi M. T., Effects of hydrolysis processing on the characterization of forsterite gel fibers. Part I: preparation, spinnability and molecular structure. *J. Eur. Ceram. Soc.*, 2002, **22**(7), 1073–1083.
12. Kamiya, K. and Yoko, T., Synthesis of SiO_2 glass fibers from $Si(OC_2H_5)_4$–H_2O–C_2H_5OH–HCl solutions through sol-gel method. *J. Mater. Sci.*, 1986, **21**, 842–848.
13. Orcel, G., Phalippou, J. and Hench, L. L., J. Structural changes of silica xerogels during low temperature dehydration. *J. Non-Cryst. Solids.*, 1986, **88**, 114–130.
14. Nogami, M., Ogawa, S. and Nagasaka, K., Preparation of cordierite glass by the sol-gel process. *J. Mater. Sci.*, 1989, **24**, 4339–4342.
15. Doeuff, S., Henry, M., Sanchez, C. and Livage, J., Hydrolysis of titanium alkoxides: modification of molecular precursor by acetic acid. *J. Non-Cryst. Solids.*, 1987, **89**, 206–216.
16. Nakamoto, K., *Infrared and Raman Spectra of Inorganic and Coordination Compounds*, 4th edn.. John Wiley & Sons, New York, 1986 (pp. 231–233).
17. Yoko, T., Kamiya, K. and Tanaka, K., Preparation of multiple oxide $BaTiO_3$ fibers by the sol-gel method. *J. Mater. Sci.*, 1990, **25**, 3922–3929.
18. Mazza, D., Lucco-Borlora, M., Bussa, G. and Delmastro, A., High-quartz solid-solution phases from xerogels with composition $2MgO$–$2Al_2O_3$–$5SiO_2$ (μ-Cordierite) and Li_2O–Al_2O_3–$nSiO_2$ ($n=2$ to 4) (β- Eucryptite): characterization by XRD, FTIR and surface measurements. *J. Eur. Ceram. Soc.*, 1993, **11**, 299–308.
19. Gabelica-Robert, M. and Trate, P., Vibrations spectrum of akermanite-like silicates and germanates. *Spectrochimica Acta*, 1979, **35A**, 649–654.
20. Sales, M. and Alarcon, J., Crystallization of sol-gel-derived glass ceramic powders in the CaO–MgO–Al_2O_3–SiO_2 system. *J. Mater. Sci.*, 1994, **29**, 5153–5157.
21. Farmer, V. C., *The Infrared Spectra of Minerals*. Mineralogical Society, London, 1974 (pp. 475-476).
22. Powder diffraction File, Card No. 34-189, JCPDS International Center for Diffraction Data, Swarthmore, PA, 1993.
23. Powder diffraction File, Card No. 4-829, JCPDS International Center for Diffraction Data, Swarthmore, PA, 1992.
24. Binker, C. J., Hydrolysis, condensation of silicates; effects on structure *J. Non-Cryst. Solids.*, 1988, **100**, 31–50.
25. Mendelson, M. I., Average grain size in polycrystalline ceramics. *J. Am. Ceram. Soc.*, 1969, **52**, 443–446.
26. Sakka, S. and Kamiya, K., Glasses from metal alcoholates. *J. Non-Cryst. Solids*, 1980, **42**, 403–422.
27. Kitaoka, K., Takahara, K., Kozuka, H. and Yoko, T., Sol-gel processing of transparent PLZT ((Pb, La) (Zr, Ti) O_3) fibers. *J. Sol-Gel Sci. Technol.*, 1999, **16**, 183–193.
28. Dislich, H., Glassy and crystalline systems from gels: chemical basis and technical application. *J. Non-Cryst. Solids*, 1983, **57**, 371–388.
29. Lacourse, W. C., Continuous filament fibers by the sol-gel processes. In *Sol-Gel Technology for Thin Films, Fibers, Preforms, Electronics, and Specialty Shapes*, ed. L. C. Klein. Noyes Publications, New Jersey, 1988, pp. 184–198.